# Evaluation of a Commercial-Off-The-Shelf dual-frequency GPS receiver for use on LEO satellites

Jan Leyssens, *Septentrio NV, Belgium*

Markus Markgraf, *Deutsches Zentrum fur Luft- und Raumfarth (DLR), German Space Operations Center (GSOC)*

## BIOGRAPHY

*Jan Leyssens* graduated in 2003 as a *Master in Industrial Sciences – Electronics Design* from Group-T Institute of Technology (Leuven, Belgium). Recently he also obtained a *Master in Industrial Sciences – Avionics*, an advanced part-time study, from the KHBO, Department of Industrial Sciences & Technology (Ostend, Belgium) After working as an Application Engineer at ST-Microelectronics for one year, he joined Septentrio as a software design engineer. He is responsible for working on the PolaRx2 firmware design.

*Markus Markgraf* is a GPS development engineer at DLR/GSOC. He has prepared and conducted various sounding rocket flight experiments at Esrange, Kiruna. He was in charge of the preparation of a number of space missions with GPS receivers onboard. He also has specialized in environmental and signal simulator testing of GPS receivers.

## ABSTRACT

Testing and qualification of commercial receivers for space applications is done by the DLR on a regular basis. In this paper we report the results of the tests performed with the Septentrio's PolaRx2 dual-frequency GPS receiver. In order to qualify for space missions, the receiver must show robustness to radiation exposure typical for low-Earth orbits, it must survive vibrations typical for launches, and demonstrate successful operation at altitudes and speeds typical for satellite platforms.

The PolaRx2 receiver has been extensively tested in signal simulator tests using a STR4760 simulator. For the tests representative of actual dynamic conditions of low-orbit satellites, the receiver have demonstrated reliable acquisitions with cold-start time of a few minutes, robust tracking and the accuracy of measurements similar to its normal terrestrial performance.

During environmental tests the receiver was also subjected to a total ionizing dose radiation test to verify its ability to survive for a few years on low-Earth orbits. The test results are comparable to those obtained earlier for other commercial receivers and demonstrate general suitability for low-Earth orbits.

Results from random and sinusoidal vibration tests indicate that the PolaRx2 is able to survive a launch on several types of launchers. A first flight test with the PolaRx2 receiver onboard a technology demonstration micro-satellite is currently planned for 2008 as part of DLR's On-Orbit Verification Program.

## INTRODUCTION

Small-scale satellite projects have become affordable for universities and research organizations; they typically use small satellites as technology demonstrator, for short duration Earth observation missions or for educational purposes. Dedicated space-certified GPS receivers may cost a considerable portion of the project budget due to the expensive space-qualification process of the receiver. Commercial-Off-The-Shelf (COTS) technology is an interesting alternative due to lower cost. Due to the relatively low altitudes and short durations of research/education missions, requirements to their radiation resistivity are not so stringent as for the dedicated space receivers.

However, commercial geodetic-grade GPS receivers are not designed with space applications in mind; the harsh space environment places a heavy burden on them. Therefore it needs to be investigated whether a receiver can survive these conditions. Furthermore, the GPS signal acquisition in regular GPS receivers is optimized for use on or near the Earth's surface, and SW modifications to tracking/acquisition algorithms may be required to make them suitable to use in orbit.

The German Aerospace Center (DLR) has gained significant experience with qualifying COTS GPS receivers for use in space. Currently the DLR has teamed up with Septentrio Satellite Navigation, Belgium to

qualify and test their dual-frequency receiver, the PolaRx2, for use in space applications.

## DUAL-FREQUENCY GPS RECEIVERS IN SPACE

Similar to terrestrial applications, dual-frequency GPS receivers offer numerous advantages over single-frequency receivers in space applications. Even though single-frequency receivers can easily meet the basic navigation requirements of many spacecraft, the availability of the second frequency is of great interest for scientific missions, in particular for high-accuracy post-mission positioning and radio occultation measurements.

The CHAMP mission, which carries a US-built BlackJack receiver, is a prominent example of such an application. Availability of precise GPS observations from the CHAMP satellite has dramatically improved our knowledge of the Earth gravity field. GPS based radio occultation measurements from CHAMP are an indispensable source of information for ionospheric and tropospheric research.

In carrier-phase differential GPS, dual-frequency measurement enables a reliable resolution of integer ambiguities even at large baselines and non-negligible ionospheric delays. This has recently been demonstrated for the GRACE formation with a spacecraft separation of about 200km. The relative position of two satellites could be determined with a 1mm-accuracy, which paves the way for future formations, e.g., TanDEM-X.

As the existing space-qualified dual-frequency GPS receivers are quite expensive, using commercial dual-frequency receivers could be an interesting alternative for low-cost satellite missions.

## POLARX2 GPS RECEIVER

Septentrio Satellite Navigation, Leuven, Belgium, designs, manufactures, markets and supports high-end OEM GPS/GNSS receivers for precise navigation, positioning and timing applications. Septentrio's main product is the PolaRx2 dual-frequency GNSS receiver.

The PolaRx2 is a general-purpose 48-channel dual-frequency GNSS receiver for high-end OEM applications. It is built around the GReFE (GNSS front-end) and the GReCo (GNSS Receiver Core) GPS/SBAS baseband processor chips. Core computations are performed on a MachZ "system-on-a-chip" computer that includes an i486 core with PCI and serial interfaces.

**Figure 1: The PolaRx2@ OEM-board**

The 48 channels of PolaRx2 can be configured to track C/A code, P1 code and P2 code for up to 16 GPS satellites. There also exists a multi-antenna version, the PolaRx2@, that provides measurements from multiple antennas in a mixed single/dual-frequency configuration. The PolaRx2@ can also be used to provide real-time attitude information.

Although the PolaRx2 appeared in the market only in 2003, but it was already used in many research projects and gained a reputation for its low noise characteristics, configurable channel architecture, user-friendly interface and high quality of user support. The purpose of this testing was to determine its suitability for low-orbit space applications.

## PERFORMANCE ANALYSIS

With most GPS receivers, the implemented positioning and tracking algorithms are not able to work in a satisfactory manner when used on a satellite in orbit. Due to the high values of speed and acceleration in low-Earth orbits, modifications are needed, so that the receiver could acquire and track the GPS satellites from space. On orbits with an altitude of 500 km, a satellite has a velocity of ±7000 m/s. This introduces a Doppler shift of roughly 36 kHz, so if the search window of the receiver acquisition process is not enlarged, most terrestrial receivers would have difficulties in acquiring the GPS satellites. Also the fast acquisition of satellites after a reboot is more difficult. On Earth, the last computed position/time can be used to speed up the acquisition, assuming that the vehicle's speed is negligible with respect to the GPS satellite's motion. When flying on a satellite that is traveling with a velocity of 7000 m/s, this assumption is obviously not valid. To analyze the signal acquisition and the navigation performance, extensive testing has been completed using a Spirent STR4760 dual-frequency 8-channel GPS signal simulator.

In accordance with applicable European export restrictions, the PolaRx2 receiver normally prohibits the output of valid data at heights greater than 18km and at speeds greater than 515 m/s. In order to allow assessment of the operation in orbit, a special firmware has been made with these limits removed. In addition, the frequency search window has been extended to facilitate the acquisition of GPS signals from a satellite platform.

**Simulated Scenario**

To assess the tracking performance of a spaceborne GPS receiver, the Spirent simulator generates artificial GPS signals, which closely match the real signals in orbit. The scenario is configured for a spacecraft orbiting the Earth in a near polar-orbit of 450 km altitude, 87 degrees inclination and an eccentricity of 0.001. This resembles the orbits of the CHAMP and GRACE satellites. The epoch which coincides with the ascending crossing of the equator, is chosen at 6 November 2001, 0:00 GPS time, i.e. the beginning of day 2 in GPS week 1139. Consistent with this epoch, the GPS constellation was modeled based on the actual almanac data from GPS week 1138. All relevant information can be collected during a simulation run of 2 hours, enough to simulate at least one Earth orbit. [1]

During the first test, an ionosphere free simulation was used in order to get a clear understanding of the performance of the PolaRx2 in an error-free condition. In a second simulation, the vertical total electron content (VTEC) will be set to 20 TECU ($2.10^{17}$ electrons/$m^2$). During these simulations, multipath and broadcast ephemeris errors were set to 0. The recording data rate was 1Hz.

The measurements output by the PolaRx2 are, by default, obtained from the quadratic polynomial fitted to raw samples. When this fitting is used, the measurement noise is significantly reduced. For the first two simulations, the measurement fitting was disabled in order to assess the quality of the raw data generated by the receiver. The third simulation was done with the measurement fitting enabled.

**Time-to-first-fix (TTFF)**

Normally, at start-up, the PolaRx2 calculates the visibility of each satellite based on information stored in the non-volatile memory of the receiver: (1) the latest position computed by the PolaRx2; (2) the latest received almanacs and ephemeris; (3) the elevation mask setting; (4) the current time retrieved from the real-time clock. This information might be incorrect if the receiver has moved over a significant distance or if the latest stored orbit data is outdated. If the PolaRx2 fails to acquire a satellite within 45 seconds after start-up, or after a cold-start, it enters a full-sky search mode in which it starts acquisition of all the GPS satellites sequentially until it succeeds in computing a position. During this process all 48 hardware channels are used for acquiring the C/A code.

The initial acquisition performance was assessed during one of the simulator tests. A ‘reset all’ command was sent to the receiver, which caused the PolaRx2 to erase all the data in non-volatile memory and to restart the receiver into the default boot configuration. This is also called a cold-start of the receiver.

After a reset, the PolaRx2 locked to the C/A code of the first GPS satellite after a few seconds followed by the P-code acquisition. For a dual-frequency 3D navigation, four tracked satellites and the successful decoding of the respective navigation messages are needed. This test has been repeated several times and a average TTTF of 154 seconds has been calculated with a standard deviation of 31sec.

Although an acquisition time of about 2.5 minutes is sufficient for a spaceborne receiver, investigations are underway in order to improve the cold-start performance of the receiver. This can, for example, be achieved by implementing an orbital model that calculates a rough position to aid the acquisition. [1][2]

**Navigation accuracy**

The accuracy of the position and velocity solution computed by the PolaRx2 receiver has been determined with and without ionospheric errors.

The navigation accuracy analysis is based on a comparison with the reference trajectory output of the simulator.

Analysis of the status information provided by the receiver during the test shows that it was flawlessly working in a dual-frequency standalone mode and that, most of the time, all 8 simulated satellites were tracked. Figure 2 shows the errors of the position solution and Figure 3 shows the velocity errors.

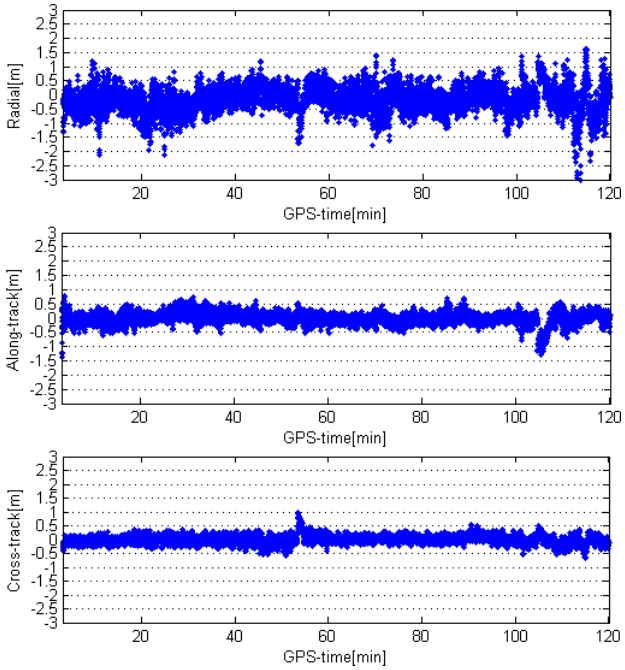


**Figure 2: Position errors relative to the simulated values**

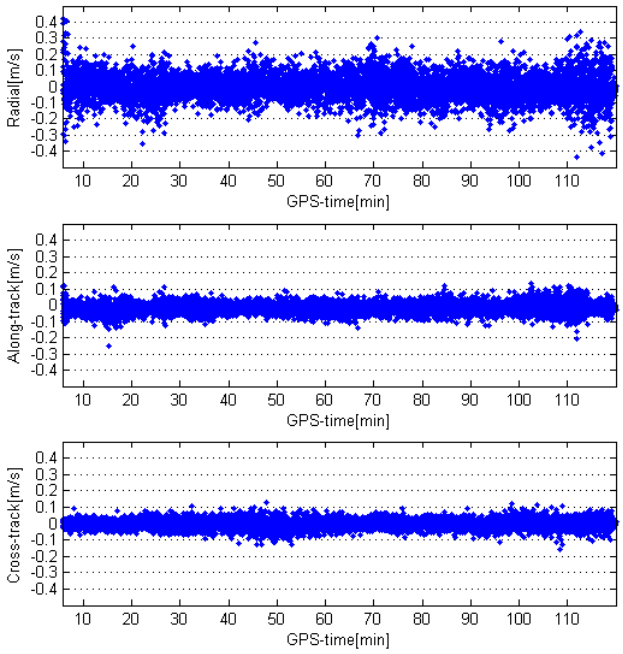


**Figure 3: Velocity errors relative to simulated values**

**Table 1: Errors on the position solution**

| Simulation | Radial [m] | Along-track [m] | Cross-track [m] |
|---|---|---|---|
| Iono-free | -0.167 ± 0.470 | -0.014 ± 0.216 | - 0.003 ± 0.169 |
| Iono-free, Measfit on | -0.081 ± 0.458 | -0.003 ± 0.220 | - 0.040 ± 0.181 |
| Iono-error | -0.210 ± 0.512 | 0.020 ± 0.204 | -0.052 ± 0.187 |

This data clearly indicate that the PolaRx is capable to calculate the position to sub-meter accuracy in situation where ephemeris and multipath errors are negligible. The second test shows that the measurement fitting improves the accuracy of the navigation solution. The fact the performance with and without ionospheric delays is practically the same indicates that the PolaRx handles ionospheric delays correctly.

First tests revealed that the velocity solution contained discontinuities, which were attributed to a bug in the velocity calculation. After fixing the issue, no systematic errors on the velocity solution were observed (see Figure 3). Similar results are obtained when ionospheric delays were incorporated into the simulation.

**Table 2: Errors on the velocity solution**

| Simulation | Radial [m/s] | Along-track [m/s] | Cross-track [m/s] |
|---|---|---|---|
| Iono-free | -0.004±0.132 | -0.018±0.033 | -0.003±0.028 |

These results clearly indicate that the PolaRx2 is capable to accurately calculate the position and velocity of spacecraft in the simulated low-Earth orbits.

## Raw data accuracy

Assessment of the raw measurement accuracy of the PolaRx2 is based on calculating double-differences between observed and simulated data for selected PRN pairs. After the raw measurements are collected, modeled pseudoranges and range rates are computed based on the simulated spacecraft trajectory and the known GPS constellation almanac. These are subtracted from the measurements to take into account the variation of the distances between the receiver and the GPS satellites. This process is shown in Figure 4. [1]

The result is essentially the sum of the receiver and simulator clock errors and measurement noise. To eliminate the dominating clock terms, the measurements of both channels are differenced again. This results in a zero-mean white-noise sequence with a variance equal to the sum of the noise variances of individual satellites.

For two channels with similar signal-to-noise ratios, the noise errors are expected to be of equal size and the r.m.s. noise of the inter-channel difference is $\sqrt{2}$ times as high as the noise of the un-differenced measurements. It should be stressed that this test can be used to detect biases related to signal dynamics and other satellite-related effects because only one receiver is involved (these effects are canceled in a classical zero-baseline test setup with 2 receivers).

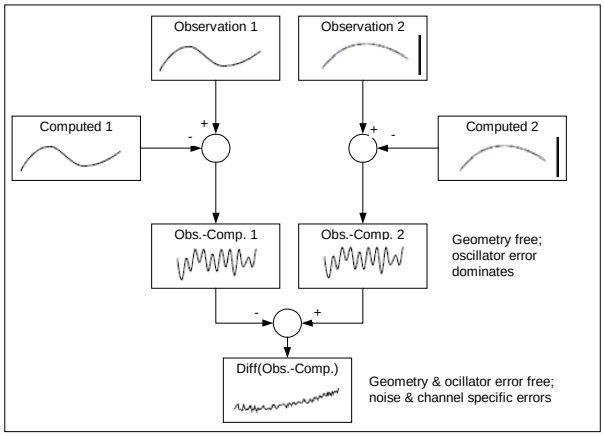


**Figure 4: Double differencing observations with computed values**

Suitable time intervals and pairs of PRNs, which offer either similar or widely different signal dynamics, are presented in Table 3. These combinations are used for both the raw measurement analysis and the zero-base line test, which will be described later on.

**Table 3: Recommended double difference combinations**

| # | PRNs | Start | End | Description |
|---|---|---|---|---|
| 1 | 2-28 | 174000s | 175800s | Low relative dynamics ([-0.5, 0.0] km/s, ±0.05g), high signal level |
| 2 | 14-29 | 178100s | 180000s | Low relative dynamics([-2,0] km/s, ±0.2g), high signal level |
| 3 | 3-15 | 177400s | 178900s | Low relative dynamics(±1km/s, ±0.2g), medium signal level |
| 4 | 21-28 | 173800s | 174700s | High relative dynamics([8,10] km/s, ±1g), high signal level |
| 5 | 13-22 | 176500s | 177700s | High relative dynamics([3,8] km/s, ±1g), high signal level |
| 6 | 6-17 | 177100s | 178000s | High relative dynamics([4,7] km/s, ±0.8g), medium signal level |

The standard deviations of the double differences obtained from this test are collated in Table 4. The individual data types are labeled with RINEX identifiers: C1, P1, P2 for pseudoranges; L1, L2 for carrier phases; D1, D2 for Doppler measurements.

**Table 4: Standard deviations double differences**

| **No ionospheric errors** | | | | | | | | |
|---|---|---|---|---|---|---|---|---|
| **#** | **PRN** | **C1** | **L1** | **P1** | **D1** | **P2** | **L2** | **D2** |
| 1 | 2 28 | 0.15 m | 0.81 mm | 0.10 m | 0.037 m/s | 0.12 m | 1.15 mm | 0.037 m/s |
| 2 | 14 29 | 0.15 m | 0.89 mm | 0.11 m | 0.044 m/s | 0.10 m | 1.32 mm | 0.044 m/s |
| 3 | 3 15 | 0.17 m | 0.97 mm | 0.12 m | 0.051 m/s | 0.11 m | 1.56 mm | 0.061 m/s |
| 4 | 21 28 | 0.17 m | 1.09 mm | 0.12 m | 0.040 m/s | 0.11 m | 1.73 mm | 0.040 m/s |
| 5 | 13 22 | 0.20 m | 1.29 mm | 0.11 m | 0.046 m/s | 0.12 m | 1.87 mm | 0.046 m/s |
| 6 | 6 17 | 0.18 m | 1.11 mm | 0.14 m | 0.055 m/s | 0.10 m | 1.98 mm | 0.055 m/s |
| **No ionospheric errors – measurement fitting enabled** | | | | | | | | |
| **#** | **PRN** | **C1** | **L1** | **P1** | **D1** | **P2** | **L2** | **D2** |
| 1 | 2 28 | 0.15 m | 0.28 mm | 0.11 m | 0.001 m/s | 0.11 m | 1.18 mm | 0.002 m/s |
| 2 | 14 29 | 0.16 m | 0.44 mm | 0.12 m | 0.005 m/s | 0.11 m | 1.14 mm | 0.005 m/s |
| 3 | 3 15 | 0.18 m | 0.45 mm | 0.12 m | 0.008 m/s | 0.10 m | 1.46 mm | 0.008 m/s |
| 4 | 21 28 | 0.16 m | 0.71 mm | 0.12 m | 0.002 m/s | 0.14 m | 1.67 mm | 0.002 m/s |
| 5 | 13 22 | 0.18 m | 1.04 mm | 0.18 m | 0.003 m/s | 0.12 m | 1.89 mm | 0.004 m/s |
| 6 | 6 17 | 0.18 m | 0.66 mm | 0.16 m | 0.008 m/s | 0.16 m | 1.76 mm | 0.008 m/s |
| **Ionospheric error, VTEC = 20 TECU** | | | | | | | | |
| **#** | **PRN** | **C1** | **L1** | **P1** | **D1** | **P2** | **L2** | **D2** |
| 1 | 2 28 | 0.15 m | 1.06 mm | 0.11 m | 0.017 m/s | 0.09 m | 1.55 mm | 0.017 m/s |
| 2 | 14 29 | 0.14 m | 1.04 mm | 0.10 m | 0.023 m/s | 0.10 m | 1.45 mm | 0.023 m/s |
| 3 | 3 15 | 0.17 m | 1.13 mm | 0.09 m | 0.024 m/s | 0.09 m | 1.70 mm | 0.024 m/s |
| 4 | 21 28 | 0.19 m | 1.39 mm | 0.12 m | 0.018 m/s | 0.10 m | 2.04 mm | 0.017 m/s |
| 5 | 13 22 | 0.20 m | 1.51 mm | 0.12 m | 0.022 m/s | 0.14 m | 2.24 mm | 0.022 m/s |
| 6 | 6 17 | 0.18 m | 1.33 mm | 0.14 m | 0.025 m/s | 0.16 m | 2.02 mm | 0.025 m/s |

Figure 5 and Figure 6 show the double differences of the pair PRN2/PRN28 (observed-computed). Note the different noise characteristics of the C/A and P-code measurements. The latter has a pronounced auto-correlation caused by the narrow DLL. Also, at low $C/N_0$, the P-code DLL bandwidth is further reduced, leading to a potentially larger error. This can clearly be seen at the beginning and at the end of the plots. Similar results for the raw data accuracy were obtained in a test with simulated ionospheric path delays.

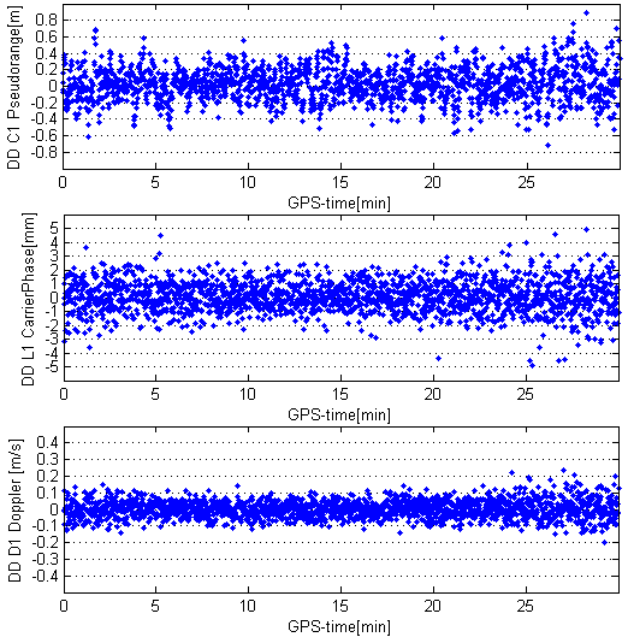


**Figure 5: Double differences (PRN2-28, observed-modeled) of PolaRx2 measurements; C1, L1 and D1.**

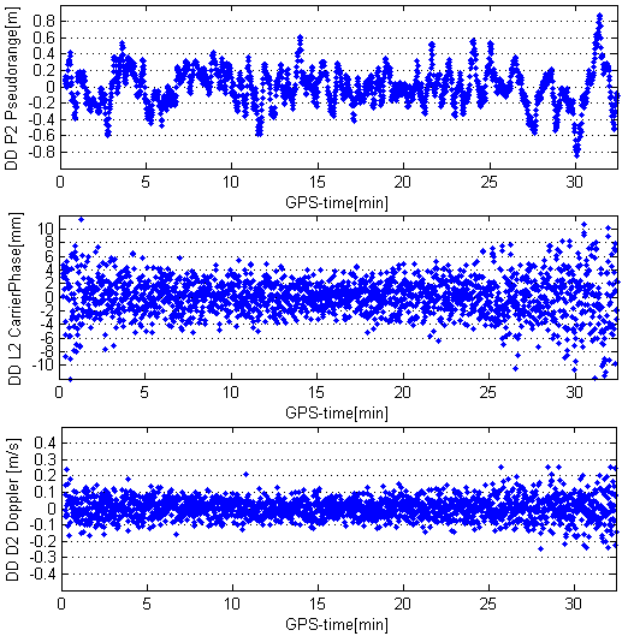


**Figure 6: Double Differences (PRN2-28, observed - modelled) of PolaRx2 measurements: P2, L2, D2**

**Interfrequency biases**

Further to the analysis of the raw data measurement noise presented in the previous section, interfrequency biases, or differential code biases (DCB), can be assessed using the same data sets. Interfrequency biases in the receiver will result in the biases of all the calculated dual-frequency combinations. For example the ionospheric delay (I=1.546*(P2-P1)) will be biased if a DCB is present. Hence it is important to know these values when using the PolaRx2 for ionospheric studies. If the bias is the same for all channels, it maps into a clock bias, so positional solutions are not affected.

Table 5 lists the interfrequency biases measured for a few satellites during the ionosphere-free scenario. As can be seen, the PolaRx2 exhibit only relatively small biases, which are PRN-independent within the accuracy of their estimation. Note the slightly different results that are applied when simulating P-code or Pseudo-Y. It needs to be investigated whether this difference is related to the simulator or the receiver.

**Table 5: Interfrequency Biases**

| PRN | P1-CA [m] | P2-CA [m] | P2-P1 [m] |
|---|---|---|---|
| **P code simulated** | | | |
| 1 | -0.283±0.165 | -0.134±0.157 | 0.149±0.152 |
| 2 | -0.304±0.123 | -0.045±0.130 | 0.214±0.132 |
| 4 | -0.295±0.136 | -0.048±0.158 | 0.246±0.150 |
| 14 | -0.304±0.120 | -0.126±0.131 | 0.178±0.120 |
| 22 | -0.304±0.107 | -0.085±0.124 | 0.390±0.095 |
| **PseudoY code simulated** | | | |
| 1 | -0.509±0.249 | -0.467±0.282 | 0.042±0.263 |
| 2 | -0.562±0.189 | -0.455±0.201 | 0.107±0.157 |
| 4 | -0.549±0.188 | -0.438±0.227 | 0.112±0.163 |
| 14 | -0.537±0.198 | -0.472±0.193 | -0.065±0.164 |
| 22 | -0.542±0.178 | -0.490±0.178 | 0.052±0.151 |

**Zero-Baseline Test**

In addition to the previously described single-receiver test, the raw measurement accuracy of the PolaRx2 has also been assessed in a traditional zero-baseline test. In this test systematic errors that are common to both receivers forming the double difference are cancelled. Hence the zero-baseline test is well suited to determine the noise level of the pseudorange, carrier phase and Doppler measurements.

For the zero-baseline test, two PolaRx2 receivers were connected to a common outlet of the signal simulator via a splitter. (Figure 7) The same error-free scenario has been used for this test. In order to compensate for the loss in signal power level introduced by the splitter and the DC-blocker, the signal simulator output power was raised to match real-life signal-to-noise ratios. Measurement fitting was disabled on both receivers

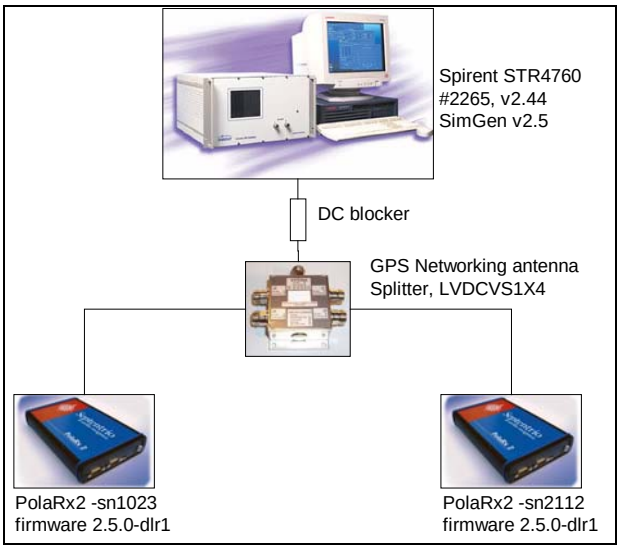


**Figure 7: Test setup zero-baseline tests**

In a zero-baseline test, the measurement noise is assessed by computing double-differences between the two receivers and between the pairs of satellites with similar signal-to-noise ratios. Because all the errors caused by external factors and also the systematic errors are cancelled, the result of this calculation will be the thermal noise of the receivers. In order to obtain the noise estimation referred to one satellite and one receiver, the resulting RMS error must be divided by 2 assuming that both satellites and receivers have same noise values.

Table 6 lists the results of the zero-baseline test. A good agreement between simulations with and without ionospheric delays can be observed.

**Table 6: Zero-baseline results**

| **No ionospheric errors** | | | | | | | | |
|---|---|---|---|---|---|---|---|---|
| **#** | **PRN** | **C1 [m]** | **L1 [mm]** | **P1 [m]** | **D1 [m/s]** | **P2 [m]** | **L2 [mm]** | **D2 [m/s]** |
| 1 | 2 28 | 0.15 | 0.84 | 0.11 | 0.030 | 0.12 | 1.46 | 0.030 |
| 2 | 14 29 | 0.16 | 0.86 | 0.11 | 0.035 | 0.11 | 1.35 | 0.035 |
| 3 | 3 15 | 0.17 | 0.94 | 0.11 | 0.040 | 0.12 | 1.50 | 0.040 |
| 4 | 21 28 | 0.22 | 1.06 | 0.21 | 0.040 | 0.17 | 1.98 | 0.040 |
| 5 | 13 22 | 0.18 | 0.94 | 0.12 | 0.035 | 0.13 | 1.58 | 0.035 |
| 6 | 6 17 | 0.18 | 1.04 | 0.15 | 0.040 | 0.11 | 1.88 | 0.040 |
| **Ionospheric error, VTEC =20 TECU** | | | | | | | | |
| **#** | **PRN** | **C1 [m]** | **L1 [mm]** | **P1 [m]** | **D [m/s]** | **P2 [m]** | **L2 [mm]** | **D2 [m/s]** |
| 1 | 2 28 | 0.15 | 1.04 | 0.11 | 0.015 | 0.12 | 1.59 | 0.015 |
| 2 | 14 29 | 0.15 | 0.85 | 0.10 | 0.035 | 0.11 | 1.28 | 0.035 |
| 3 | 3 15 | 0.17 | 0.97 | 0.09 | 0.040 | 0.11 | 1.56 | 0.040 |
| 4 | 21 28 | 0.19 | 1.04 | 0.11 | 0.015 | 0.11 | 1.58 | 0.015 |
| 5 | 13 22 | 0.18 | 1.05 | 0.13 | 0.045 | 0.13 | 1.83 | 0.045 |
| 6 | 6 17 | 0.17 | 1.11 | 0.14 | 0.045 | 0.15 | 1.95 | 0.045 |

Differences between the PRN pairs can be attributed to the different relative signal dynamics for each of the PRN pairs, as listed in Table 3.

## TID RADIATION TEST

Although the Earth's magnetic field offers some protection for satellites in low-Earth orbits, the charged particles trapped by the magnetic field can still damage some components of the receiver, especially commercial components such as memory chips, oscillators and processors. In order to assess the resistivity of the PolaRx2 receiver, two types of tests have been defined: Total Ionizing Dose (TID) tests and Single Event Effect (SEE) tests. At this moment, only the TID test has been performed. In these tests, not only some key electrical parameters are monitored, as in traditional radiation tests, but also the performance under realistic signal conditions is tested.

During the tests, the receiver under test is connected to an outside antenna and the second PolaRx2 reference receiver, which is situated outside of the radiation chamber, is operated in a zero-baseline configuration to allow a qualitative and quantitative assessment of the impact of the radiation on the performance of the GPS receiver.

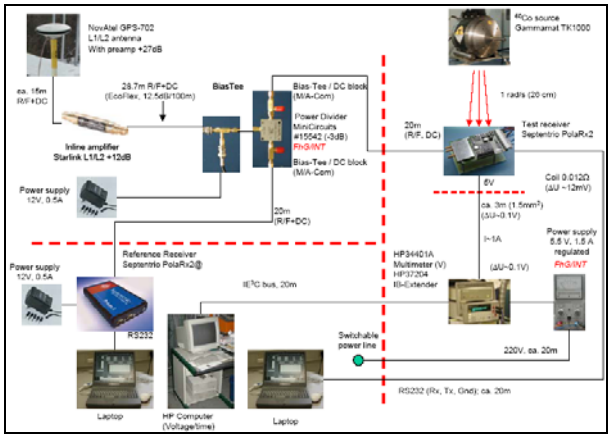


**Figure 8: Test Setup**

The TID test has been conducted at the Fraunhofer Institute For Technological Trend Analysis (FhG/INT) in Euskirchen, Germany. A Gammamat TK1000 Cobalt-60 radiation source was used to irradiate the receiver with a dose 1 rad/s referred to the center of the receiver board. Throughout the exposure, the PolaRx2 supply current was monitored to assess the expected increase in power consumption over the mission lifetime. Data was logged from the two receivers in the zero-baseline configuration in order to reveal any influence of radiation on the performance of the receiver. To validate the proper function of the receiver memory and boot process, the PolaRx2 was power-cycled at specified intervals (every 2 kRad).

Results from this test have shown that the PolaRx2 continued to function correctly until a total accumulated dose of ±9,4 kRad was reached. At this dose, the reference oscillator, which is used to generate a clock signal for the processor, failed to generate a clock output. When the processor lost its clock, the PolaRx2 stopped functioning. However, the day after the test, the oscillator was operating normally again.

**Figure 9: The PolaRx2 below the Gammamat TK1000 at the test facility of FhG/INT, Euskirchen**

As the radiation dose that was used (1 rad/sec) is significantly higher than can be anticipated on low-Earth orbits, it is to be expected that the PolaRx2 will survive much longer in a real-life application due to self-healing properties of semi-conductor devices. Nevertheless we are looking at alternatives to replace the oscillator by a more radiation-resistive component.

### Supply Current

In general, the variation of the supply current observed during a TID test provides a direct indication of the radiation-induced component aging in electronic systems. It reflects the occurrence of leak currents that ultimately result in a destruction of the irradiated device. Figure 10 illustrates the current consumption of the radiated receiver as a function of accumulated TID.

The first plot shows the current consumption of the radiated receiver. As can be seen, the supply current varies with the number of tracked satellites, as the number of hardware channels used in the GReCo changes. In order to investigate the influence of the radiation on the supply current, changes related to the number of tracked satellites have been removed.

Starting from 5 kRad, a slight increase in supply current can be observed. This might indicate that the electronics are influenced by the radiation. However the difference between the current consumption at the start of the test and the one at the end of the test is very small and is much less than 1%.

The supply current measurements give all indications that the PolaRx2 is quite resistant to effects caused by TID accumulation. However, only the total current has been monitored, so some individual low-power components might still experience dramatic current increases, relative to their normal level of consumption.

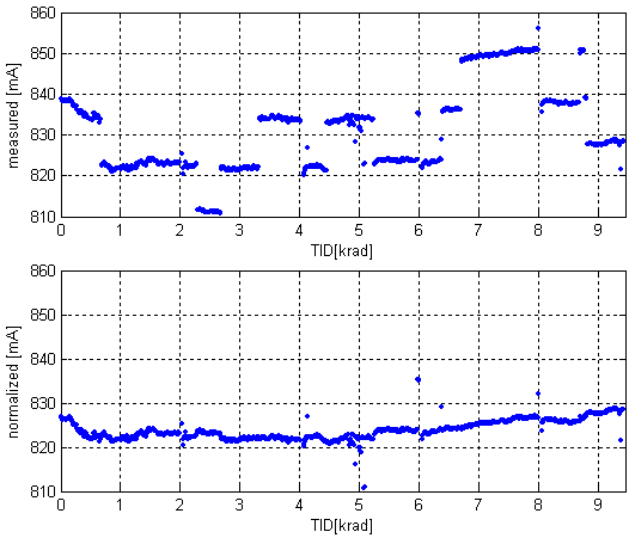


**Figure 10: Supply current radiated receiver as a function of TID**

## Clock Drift

The PolaRx2 uses a 10 Mhz temperature-compensated crystal oscillator (TCXO) as a frequency reference. Because this internal clock is less precise than the clocks onboard the GPS satellites, the receiver clock normally drifts compared to the GPS time. A fine-synchronization mode is used when the PVT is computed, and the receiver clock bias is available from the PVT solution. In this mode, the clock bias has a nanosecond-level accuracy. A clock jump of 1msec will be imposed when the receiver clock bias exceeds 0.5 milliseconds.

The receiver transmits both the value of the clock bias and the clock drift. Figure 11 shows the clock drift, which is most relevant for this analysis.

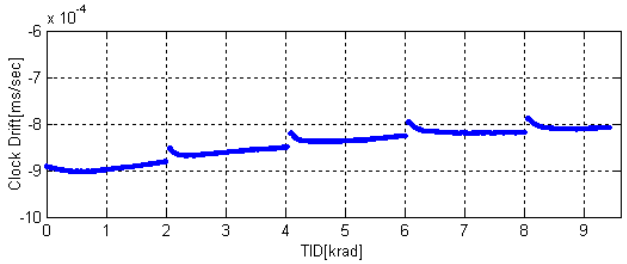


**Figure 11: Clock drift as a function of TID with transient effect after each reset.**

As the radiation dose increases, also the clock drift of the TCXO slightly changes. After each reset, a short settling period can be seen; however this is not caused by radiation effects as it is also observed in normal lab environment.

The behavior of the TCXO is better than expected. Earlier tests completed by DLR with other receivers using similar oscillators revealed more significant influence of the radiation. Further testing should be executed to find out if this good performance is consistent for other PolaRx2 receivers.

## Signal Tracking and Navigation Accuracy

Analysis of the status information contained in the data retrieved from the PolaRx2 shows that throughout the test the receiver was normally operating in a dual-frequency stand-alone mode. Most of the time, the radiated receiver was tracking the same satellites as the reference receiver. No functional degradation of the PolaRx2 could be seen.

The accuracy of the navigation solution and the overall tracking performance was evaluated by computing the position and velocity deviations from the reference position. The reference speed is 0 m/s as the antenna was fixed on the roof.

Table 7 contains the statistics for position/velocity deviations compared to the reference position. These values are normal for a standalone dual-frequency receiver.

**Table 7: Error statistics for position and velocity solution**

| Value | Mean | Stdev |
|---|---|---|
| ECEF X | 0.909 m | 0.897 m |
| ECEF Y | 0.328 m | 0.302 m |
| ECEF Z | 1.040 m | 0.844 m |
| $V_x$ | 0.028 m/s | 0.025 m/s |
| $V_y$ | 0.016 m/s | 0.015 m/s |
| $V_z$ | 0.016 m/s | 0.015 m/s |

Figure 12 and Figure 13 show the absolute errors on the position/velocity solution. Unlike some other receivers previously tested by DLR, the position and velocity solutions generated by the PolaRx2 receiver did not exhibit any outliers that would indicate instability of the tracking process as a result of the radiation exposure. After the resets, small outliers can be seen on the position and velocity solution of the radiated receivers, however it is unlikely that they have been caused by radiation influences.

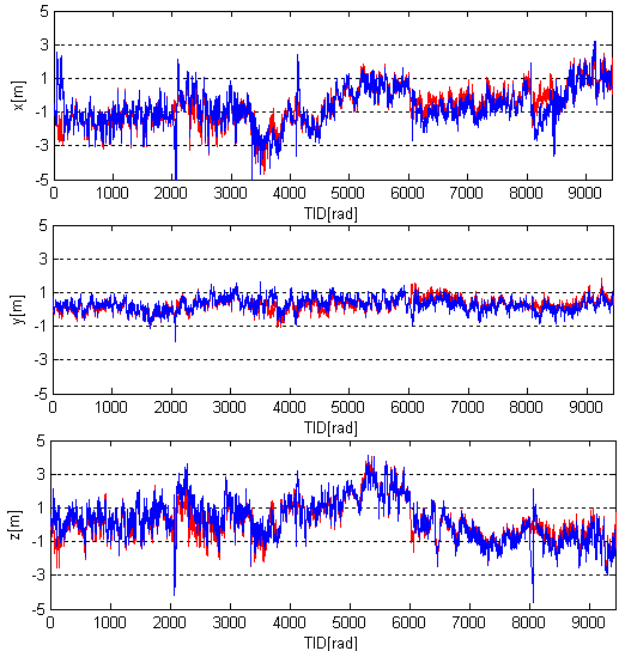


**Figure 12: Position residuals of the reference receiver (red) and the radiated receiver (blue) as function of accumulated TID**

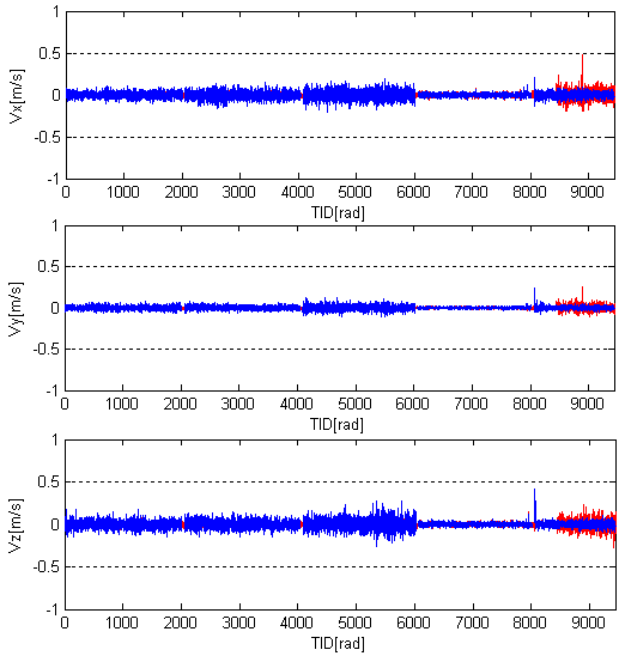


**Figure 13: Velocity residuals of the reference receiver (red) and the radiated receiver (blue) as function of accumulated TID Raw data evaluation**

As discussed before, the zero-baseline test configuration allows eliminating all the systematic errors of the raw data by forming the double differences between GPS measurements from two satellites obtained by two receivers using the same antenna. By using this method, GPS satellite errors, propagation-related errors and antenna-related errors can be eliminated. Remaining errors of the observables are caused by the receiver measurement noise.

Double differences for all measurement types have been calculated: C/A, P1 and P2 code, L1 and L2 carrier phase and D1 and D2 Doppler. Before calculating the double-difference, the time tag of the measurements is corrected for the receiver clock bias. Then, the observables are extrapolated to the nearest integer second to allow calculating the double differences.

Figure 14 shows the double differences of CA pseudorange and L1 carrier-phase measurements for the PRN 11-1 satellite pair. This satellite pair has been selected because they have similar $C/N_0$ values. Measurement fitting has been disabled on both the receivers.

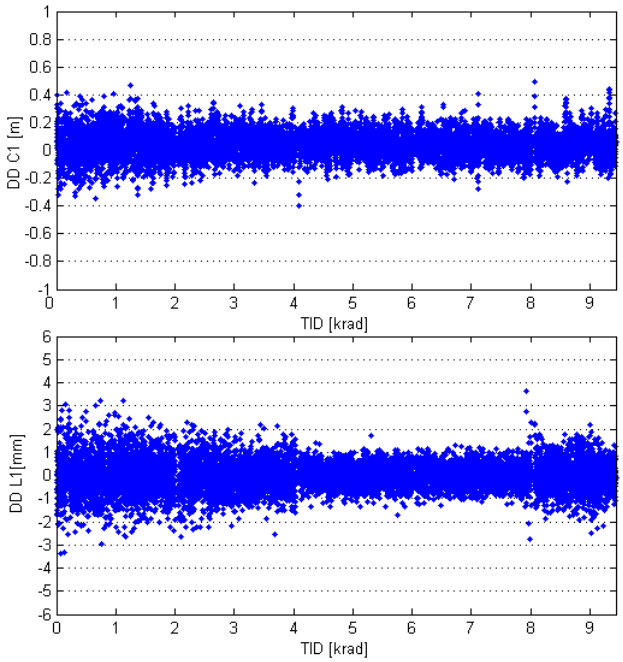


**Figure 14: Double differences of C/A code and L1 carrier-phase measurements for the PRN 11-1 satellite pair**

Table 8 lists the standard deviation of the different observables for the double difference of the PRN 11-1 satellite pair. These values are to be expected in normal operation.

**Table 8: Standard deviation double difference measurements for PRN pair 11-1 (C/A, P1 and P2 code, L1 and L2 carrier-phase, D1 and D2 Doppler).**

| Observable | Stdev |
|---|---|
| C/A | 0.071 m |
| P1 | 0.091 m |
| P2 | 0.099 m |
| L1 | 0.537 mm |
| L2 | 1.039 mm |
| D1 | 0.021 m/s |
| D2 | 0.021 m/s |

No radiation-induced errors on the raw data could be found. In particular, no cycle slips have been encountered, even at low elevation angles.

This radiation test demonstrated surprisingly high robustness of the PolaRx2 receiver against ionizing radiation despite the use of potentially sensitive electronic components. However, one should not forget that single event effects have not been assessed within the TID test. While appropriate unit level tests may be difficult to perform, a latch-up protection should certainly be considered in the design of the receiver interface electronics, to avoid the risk of receiver damage.

## VIBRATION TEST

One of the environmental tests that must be performed during the qualification of space equipment is the vibration and shock testing. A component must withstand vibration caused when launch vehicle acoustics and engine rumble are coupled to it through its structural mount.

### Random vibration

The vibration experienced is actually a random spectrum of frequencies ranging from 20 Hz to 2000 Hz. By way of example, Figure 15 shows the vibration qualification and acceptance spectra for the Chinese Long March 3 launch vehicle. The acceptance spectrum envelops the expected environment and is higher than the conducted level specified by the launch-vehicle manufacturer to account for structural resonances and acoustic input. To vibrate a component, an electromechanical shaker drives its base at a specified level of acceleration.

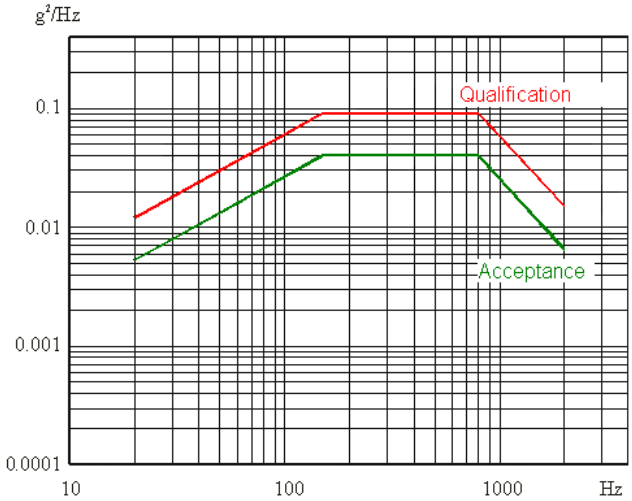


**Figure 15: Random Vibration spectrum envelope Long-March 3 rocket**

The ECSS-E-10-03A standard [4], issued by the European Cooperation for Space Standardization (ECSS), contains the vibration test level that is the envelope of the maximum expected spectra for different launch vehicles: Ariane 4, Ariane 5 and STS. Table 9 lists the random vibration test levels and duration for equipment with a mass smaller than 50 kg.

Table 10 shows the random vibration test levels that are applicable for launches with Rockot, Dnepr, Cosmos or Vega.

**Table 9: Random vibration test levels ECSS-10-03A**

| Duration | Frequency | Levels |
|---|---|---|
| All axes, 2.5 min/axis | 20-100 Hz | +3dB/octave |
| | 100 – 300 Hz | $PSD(M)^C = 0.05\,g^2/Hz \times \frac{(M+20kg)}{(M+1kg)}$ PolaRx2, packaged receiver: 720g, PSD = 0.602 g²/Hz |
| | 300 – 2000 Hz | -5dB/octave |

**Table 10: Random vibration test levels for Rockot, Dnepr, Cosmos and Vega**

| Duration | Frequency | Levels |
|---|---|---|
| Not defined | 20-100 Hz | +6dB/octave |
| | 100 – 400 Hz | 0.33 g²/Hz |
| | 400 – 2000 Hz | -6dB/octave |

Preliminary vibration tests have been performed on the PolaRx2 receiver in a standard housing. The random vibration spectrum defined by ECSS-10-03 has been used. Unfortunately, the desired maximum value exceeded the shaker's limits. The maximum acceleration reached was 0.38 $g^2$/Hz instead of 0.602 $g^2$/Hz. However this is still above the specifications listed in Table 10.

**Figure 16: The PolaRx2 in the default housing on the electromechanical shaker**

During the test, the PolaRx2 was powered down; as in most missions, the GPS receiver will only be switched on

when the satellite has left the atmosphere. The PolaRx2 was subjected to the random vibration all three directions. After each test, the operation of the receiver was verified. The PolaRx2 survived all the tests.

**Sinusoidal vibration**

Besides the random vibration test, also a sinusoidal vibration test has been performed. The purpose of sinusoidal vibration testing is to demonstrate the ability of the equipment to withstand low frequency oscillations of the launcher. During a launch sinusoidal vibrations at a single frequency will not occur. However this test provides useful information, for example to find the resonance frequency of the device and detect bad mounting techniques of components on a printed circuit board.

During the test, a sweep is performed between 5 and 100 Hz on the three axes. Table 11 lists the sinusoidal qualification test levels from ECSS-10-03A. The PolaRx2 survived all tests.

**Table 11: Sinusoidal qualification test levels, ECSS-10-03A**

| Frequency | Level |
|---|---|
| 5-20 Hz | 11 mm |
| 21-60 Hz | 20 g |
| 61-100 Hz | 6 g |

## FUTURE DEVELOPMENTS

In addition to the tests that already have been completed, thermal-vacuum testing is planned for the fourth quarter of 2005. These tests should indicate if the PolaRx2 is also able to work in vacuum conditions and at temperatures typical on a spacecraft. Shock tests should also be executed.

An effort should also be undertaken to find a replacement for the radiation-sensitive oscillator to increase the robustness of the receiver in actual flight applications. However, further studies will be required to assess the latch-up and single-event upset sensitivity under the action of high-energy radiation.

A first flight test of the PolaRx2 receiver onboard a technology demonstration micro-satellite is currently planned for 2008 as part of DLR's On-Orbit Verification (OOV) program.

## CONCLUSIONS

The PolaRx2 receiver has been extensively tested in signal simulator tests using a Spirent STR4760 simulator. Reliable acquisition with average cold-start times of <3 minutes, robust tracking and accurate measurements have been demonstrated for a low-Earth orbit simulation. These tests have also been used to determine the noise characteristics.

The total ionizing dose test results are similar to the results of other commercial dual-frequency receivers [1] and demonstrate the general suitability for use in low-Earth orbits.

Random and sinusoidal vibration tests have shown that the PolaRx2 receiver will most probably survive a launch on commonly used launchers like the Rockot, Dnepr and Cosmos and on the future European Vega launcher.

The tracking performance and the large number of channels make the PolaRx2 receiver an ideal candidate for low-budget geodetic space missions. Even with additional qualification testing, redundancy concepts and protection mechanism that are advisable when using COTS technology in space, a cost saving by a factor of 5 can still be expected compared to existing space receivers. The first flight test of the PolaRx2 is currently planned for 2008, but the PolaRx2 has already been suggested as an alternative for the upcoming SWARM constellation.

## REFERENCES

[1] Montenbruck O., Holt G, *Spaceborne GPS Receiver Performance Testing, DLR-GSOC TN 02-04*; Deutsches Zentrum für Luft- und Raumfahrt, Oberpfaffenhofen (2002).

[2] Montenbruck O., *Performance Assessment of the NovAtel OEM4-G2 Receiver for LEO Satellite Tracking*, DLR-GSOC TN 03-05; Deutsches Zentrum für Luft- und Raumfahrt, Oberpfaffenhofen (2003).

[3] Markgraf M., Montenbruck O., Metzger S., *Radiation Testing of Commercial-off-the-Shelf GPS Technology for use on LEO Satellites*, 2nd ESA Workshop on Satellite Navigation User Equipment Technologies, NAVITEC'2004, 8-10 Dec. 2004, Noordwijk, The Netherlands (2004).

[4] *Space Engineering, Testing ECSS-E10-03A*, European Cooperation for Space Standardization, February 2002